

Estimation of Blood Flow Velocity in Coronary Arteries Based on the Movement of Radiopaque Agent

S. Yu. Sokolov^{a,b}, S. O. Volchkov^{a,b}, I. S. Bessonov^c, V. V. Chestukhin^d,
G. V. Kurlyandskaya^b, and F. A. Blyakhman^{a,b,*}

^a Ural State Medical University, Yekaterinburg, 620028 Russia

^b Ural Federal University, Yekaterinburg, 620002 Russia

^c Tyumen Cardiology Research Center, Tomsk National Research Medical Center, Russian Academy of Sciences, Tomsk, 625026 Russia

^d Sklifosovsky Research Institute of Emergency Care, Moscow, 129090 Russia

*e-mail: feliks.blyakhman@urfu.ru

Abstract—The paper discusses methodological techniques for increasing the diagnostic value of routine angiographic examinations of patients. It presents algorithms for digital processing of heart video images, which make it possible to quantitatively characterize hemodynamics in the coronary bed by determining the velocity of spread of a contrast agent through the arteries. The proposed approach includes several stages and procedures and takes account of the errors caused by the movement of the arteries due to the mechanical activity of the heart. The paper presents the results of estimating coronary blood-flow velocity in a patient with coronary heart disease, which are compared with computer simulation data. The sources of errors, ways to minimize them, and prospects for using the proposed methodology for effective angiographic diagnosis are discussed.

Keywords: coronary heart disease, angiography, radiopaque agent, coronary arteries, video image processing and analysis, blood-flow velocity, computer simulation

DOI: 10.1134/S1054661819040163

INTRODUCTION

Atherosclerosis of coronary arteries (CAs) is the most common cause of coronary heart disease (CHD). The formation of cholesterol plaques on the vessel walls forms a narrowing (stenosis) of the CA, which hinders an adequate blood supply to the myocardium and inevitably leads to decreased efficiency of the work of the heart. The correct assessment of the location, specific geometry, degree, and hemodynamic significance of stenosis determines the choice of tactics for treating patients: surgical (myocardial revascularization) or non-surgical (using medication) [1]. The search for adequate criteria for the effective treatment of coronary heart disease is an urgent task of modern cardiology [2].

One of the most common methods for characterizing the morphology of heart arteries is radiopaque angiography (in other words, coronarography). A dose of a contrast agent that is safe for human health is brought directly to the mouth of the coronary bed and is visualized by X-ray examination over several mechanical cycles of the heart. The results of angiographic examination (static images and/or video

records) enable, first of all, the determination of the area of CA lesion and in some cases its degree as a ratio of the vessel diameter before the affected area to the vessel diameter in the zone of stenosis.

Additional and important information on the significance of stenosis for myocardial perfusion can be obtained from the dynamics of blood flow through an artery. Thus, a number of publications [3–8] have described approaches for estimating coronary blood flow velocity from video records obtained during the examination of patients by computed tomography (CT), magnetic resonance tomography (MRT), or two-sided coronary angiography. In particular, the study [8] considers a method for estimation of coronary blood flow based on the combined processing of video records made when performing coronary angiography and CT.

The considered approaches have not become widely used in clinical practice, primarily due to the limited prevalence of expensive CT and MRT techniques, as well as the significant labor and time costs required for the procedures and processing of the results. The current paper discusses methodological techniques aimed at increasing the diagnostic value of the routine angiographic examination of patients, which is widely used in clinical practice. Algorithms for digital processing of heart video images are pre-

Received March 20, 2019; revised July 8, 2019;
accepted July 16, 2019

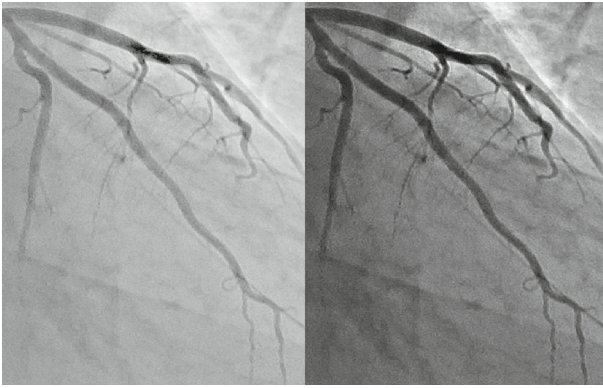


Fig. 1. Example of using local histogram alignment for the purpose of enhancing image contrast. The left part of the figure shows an original coronarogram, and its right part shows the coronarogram after processing. The branches of the left coronary artery are shown.

sented, which enable the quantitative characterization of hemodynamics in the coronary bed by determining the velocity of spread of the contrast agent front in the arteries.

The proposed approach technologically includes several stages and procedures: (1) improving the quality of video images, (2) determining the geometry of the CA, (3) recording the boundaries of the contrast agent, (4) tracking the movement of the boundaries of the contrast agent, and (5) calculating coronary blood-flow velocity. It is important to note that the algorithms presented in the study take account of the errors caused by the movement of the arteries due to the mechanical activity of the heart.

Preliminary Processing of Heart Video Images and Determining the Geometry of the Coronary Arteries

The initial data were heart video records with a frame resolution of 512×512 pixels, which were obtained during the standard procedure of angiographic examination of patients using the AXIOM ARTIS device (Siemens, Germany). At this stage, the shutter frequency was 15 frames per second. All patients were informed and gave written consent to use of the results of the examination in an impersonal form for scientific purposes.

The well-established methods of local histogram equalization and median filtering were used to improve the quality of the original video records (increasing the contrast, reducing noise, and removing artifacts) [9]. As an example, Fig. 1 shows the result of processing an original heart image by the method of local histogram equalization for one frame in the period of contrasting of the coronary arteries. It is seen that the boundaries of the arteries have acquired a clearer outline after the processing.

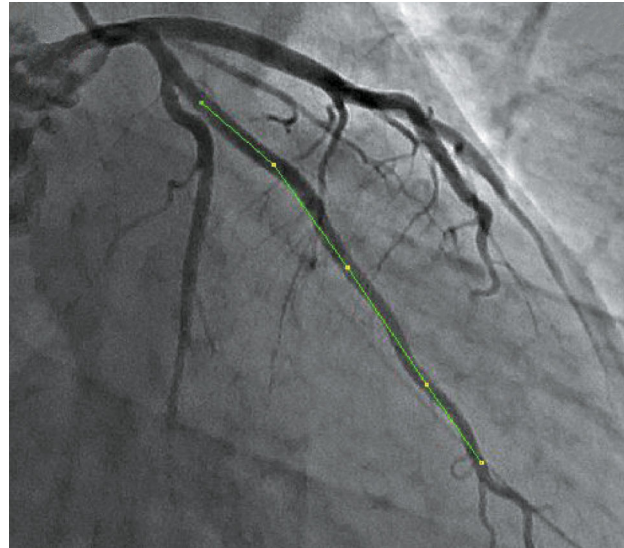


Fig. 2. (Color online) Example of constructing the initial indication of a coronary artery section for assessing vessel geometry.

The following procedure is aimed at automatic recognition of the boundaries of the CA section under study. This can be done using complex algorithms, for example, those described in the well-known study [10]. In the cited study, static images of coronarograms were initially subjected to the adaptive histogram contrasting procedure (an analogue of the procedure, see Fig. 1). Then the “region-growing” algorithm, which is the simplest iterative method of image segmentation, was used. The considered approach [10] takes into account the curvature of the artery boundaries and, if this curvature changes sharply, it decides whether there is a vessel bifurcation site and then assesses the boundaries of each branch of the CA. The method is quite computation-intensive and sensitive to noise on the images. In addition, the authors mention the requirement for a smooth reduction of the diameter of an artery without its sharp fluctuations as conditions for using this method; i.e., they impose restriction on the applicability of the method to cases of pronounced arterial stenosis.

Our study used a simpler algorithm that does not make allowance for the branching of vessels. In the context of the problem solved, there is no need for automatic determination of the boundaries for the entire vascular tree; it was enough to accurately visualize the boundaries of the problem CA with stenosis.

The considered algorithm for determining the boundaries of the vessel works as follows. First, the CA section of interest is manually indicated on the video recording frame, which corresponds to the maximum filling of the CA with the contrast agent. An example of the construction of the initial indication is shown in Fig. 2. It is important that markers be placed on the targeting trajectory with the line extending at a dis-

tance of no more than 2–3 pixels from the outer wall of the vessel.

The well-known approach described in [11, 12] was used as a basic method for automatic determination of CA boundaries. Its essence is that segments are drawn perpendicular to the line of initial indication with a certain step with the length of each of these segments being three times greater than the maximum diameter of the CA in the section under study (the diameter of the CA is set as a parameter of the method). This ensures the ratio at which the perpendicular crosses both boundaries of the vessel. The inset in Fig. 3 shows the position of one of the perpendiculars to the line that initially indi-

cates the position of the CA and the image brightness distribution along this perpendicular.

The artery border on the perpendicular was determined by fitting with the Gaussian function $g_0(x, y)$ [12], which was used as a model image brightness distribution at the vessel border. A criterion for coincidence between the position of the model brightness distribution of the vessel border and real image was the maximum of the cross-correlation function $r(\Delta x, \Delta y)$, Eq. (1). Earlier we successfully used this approach to solve similar problems [13]

$$r(\Delta x, \Delta y) = \frac{\sum_{i=-N/2}^{N/2} \sum_{j=-N/2}^{N/2} \{(g_0(x+i+\Delta x, y+j+\Delta y) - \overline{g_0})(g(x+i, y+j) - \overline{g})\}}{\sigma_0 \sqrt{\sum_{i=-N/2}^{N/2} \sum_{j=-N/2}^{N/2} (g(x+i, y+j) - \overline{g})^2}}, \quad (1)$$

where Δx and Δy are the spatial mismatch of the model (g_0) and real (g) brightness distribution; σ_0 is the standard deviation of the function g_0 ; N is the size (in both coordinates) of the image fragment, which is used to determine the vessel border (as shown in [12], the adjustable parameter must be approximately 30% of the artery diameter); and i and j are the steps of summation by x and y coordinates, respectively.

Throughout the initial targeting line (with a step of 10 pixels), the algorithm gives a description of the artery boundaries in the form of coordinates of polyline nodes. For the majority of real images, the proposed method gives a fairly accurate description of

CA boundaries. However, the accuracy of approaching the boundaries may be insufficient in the presence of noise in the image, strong crimp of the artery, as well as in places with a sharp change in the CA border (stenosis). Therefore, the method of active contours was used to better adjust the position of the border points found and decrease the interval between them [14, 15]. The essence of this method is to minimize the functional “energy” of a curved line that passes along the border of objects with a sharp brightness difference. In this case, the points of an object border (in our case, the coronary artery border) are automatically

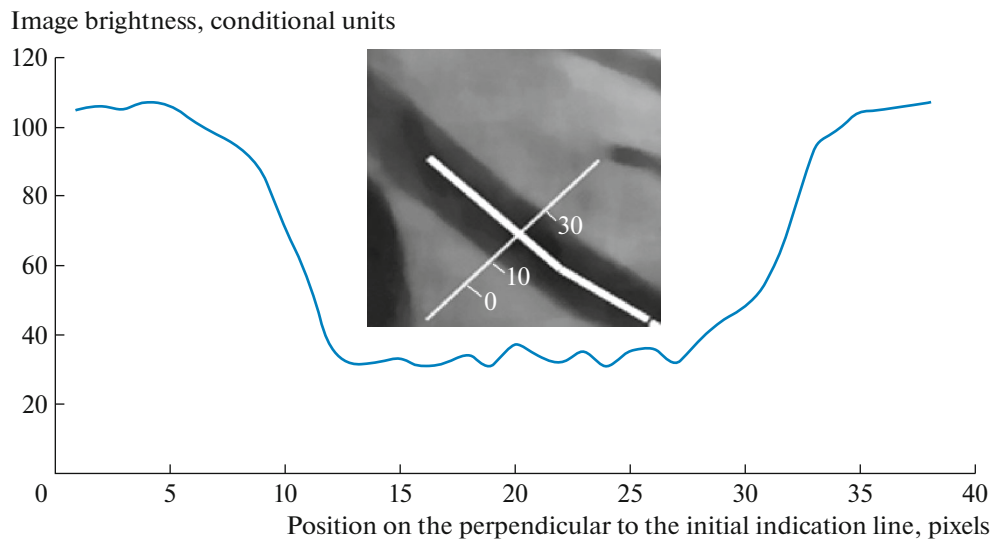


Fig. 3. (Color online) Graph of the dependence of image brightness on the position on the perpendicular to the initial indication line. The inset shows a fragment of a CA image with the initial indication line and perpendicular to it; the numbers correspond to the pixel value.

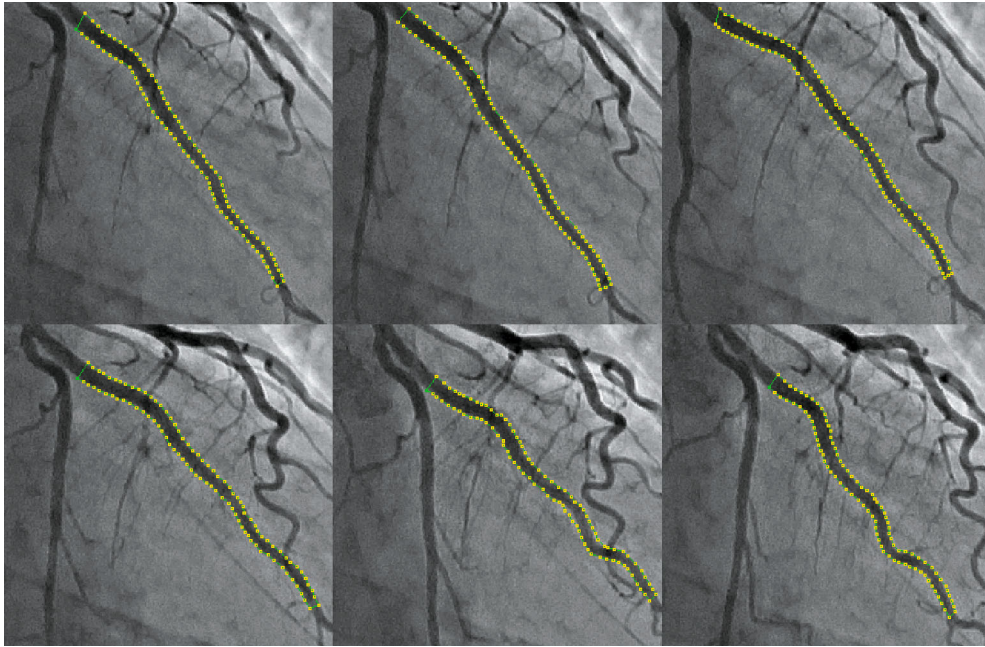


Fig. 4. (Color online) Example of frame-by-frame assessment of the coronary artery boundaries in the period of one mechanical cardiac cycle. The sequence of events is presented from left to right, from top to bottom. The first frame on the left in the upper row corresponds to the beginning of the systole of the left ventricle, and the last frame in the bottom row corresponds to the end of the diastole.

arranged so that they are as close as possible to the points of the greatest brightness gradient.

To determine the profile of the studied CA section, a central line was built and the dependence of the artery diameter as a function of distance was calculated [16]. The diameter of the vessel was determined as the length of the segment that was perpendicular to the center line of the artery and was enclosed between its boundaries.

Since the mechanical activity of the heart causes a cyclical change in the spatial configuration and shape of the coronary arteries, the geometry of the vessel of interest is assessed throughout the full cardiac cycle. The CA boundaries and vessel diameter are determined in each frame from the beginning of the mechanical contraction of the heart. Figure 4 shows the result of determining the CA boundaries for six frames of one cardiac cycle, which corresponds to the full filling of the coronary bed with the contrast agent. It can be seen that the CA geometry changes significantly by the end of the heart contraction cycle.

Thus, the methodical techniques considered in this part of the study allowed us to obtain clear contours of the CA and calculate the diameter of the areas of interest during the period of mechanical activity of the heart, i.e., during the period when the projection of the heart and configuration and diameter of the coronary arteries change significantly.

Estimation of the Velocity of Movement of the Radiopaque Agent through a Vessel

After the injection of the contrast agent into the mouth of the coronary arteries, the vessels are visually filled within approximately 0.5–1 s, after which the agent can be observed for one or two more cardiocycles. When reviewing the video frame by frame, one can see how the contrast agent spreads through the artery. Consequently, judging by the shift of the border of the contrast agent front for the interframe interval, one can get information about the blood-flow velocity in the corresponding place of the artery.

The solution of this problem has at least two important aspects that require special attention. The first aspect is the complex geometry of the CA, which depends on the mechanical activity of the heart (see Fig. 4). This greatly complicates the determination of the path covered by the contrast agent for the interframe interval. In addition, the part of the artery, which the contrast agent has not yet reached, is almost indistinguishable on video records. The second aspect is the periodic movement of the artery and change in its configuration in accordance with the phases of the mechanical cardiac cycle.

To minimize the contribution of the mentioned factors to the accuracy of determining the speed of movement of the contrast agent through the CA, the following approach was used. For each frame (F') of video recording during the period of the CA being filled with the contrast agent, the closest frame (F'')

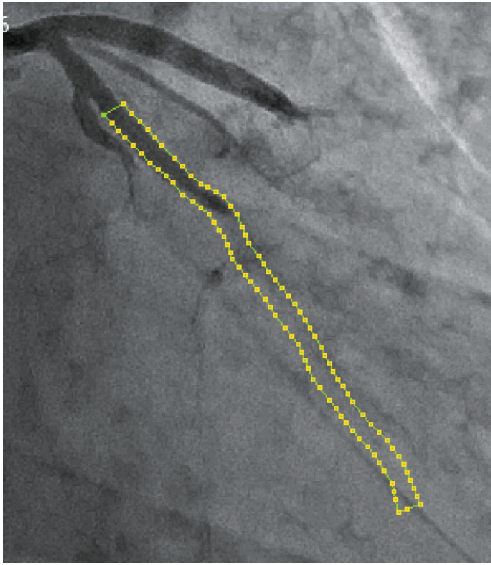


Fig. 5. (Color online) Boundaries of the coronary artery with its partial filling with the contrast agent (see explanations in the text).

was found, which was recorded during the complete filling of the artery with the contrast agent (see Fig. 4). On the one hand, this allowed the video images of the CA to be bound to the same moments of the cardiac cycle. On the other hand, it provided the correct information about the geometry of the CA at any appropriate point in time during the artery being filled with the contrast agent.

To determine the frames F' and F'' on the video records that were made at different periods of contrasting of the coronary bed, but corresponded to one

moment of the cardiac cycle, the already considered approach to calculating the cross-correlation function between image fragments in two frames was used (see Eq. (1)). Previously, we have successfully applied this technique to ultrasound diagnostics methods in order to analyze the regional movement of the heart wall [17–19] and intestinal motility [20].

Figure 5 shows a frame during the period of the CA being filled with the contrast agent, with the artery boundaries being superimposed, but defined in the corresponding frame in the case of its full filling. The figure clearly shows the border of the contrast agent in the artery, as well as the boundaries of the artery itself, for which the central line and diameter were determined at the preliminary stage.

The border of the contrast agent front was determined from a sharp difference in brightness at the center line of the CA. Figure 6 illustrates the principle of determining the border of the contrast agent in the artery. The image brightness distribution along the center line of the CA is shown (initial data and after smoothing filtering). The mean value between the averaged brightness in the artery section with the contrast agent and the averaged brightness in the section without it was taken as the threshold value for determining the border of the contrast agent.

Figure 7 shows six consecutive frames of a coronarogram, which were made during the period of the coronary bed being filled with the contrast agent. For each frame for the artery of interest, a central line is superimposed, the total length of which corresponds to the distance covered by the agent over a certain period of time. The section with a thin line corresponds to the path covered by the radiopaque agent for

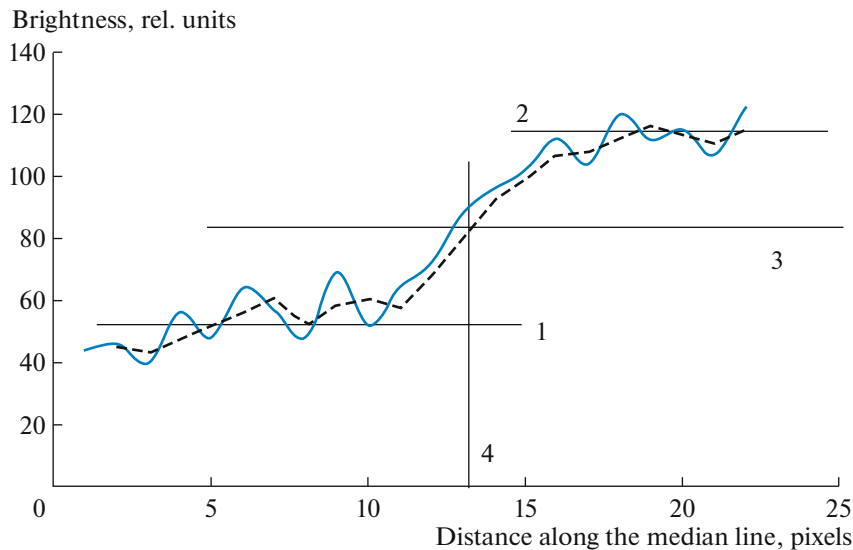


Fig. 6. (Color online) Distribution of image brightness along the center line of the CA. The solid line shows the original data, and the dotted line shows the data after smoothing. 1 is the average brightness of the CA section with the contrast agent, 2 is the average brightness of the CA section without the contrast agent, 3 is the threshold value for determining the border (4) of the contrast agent.

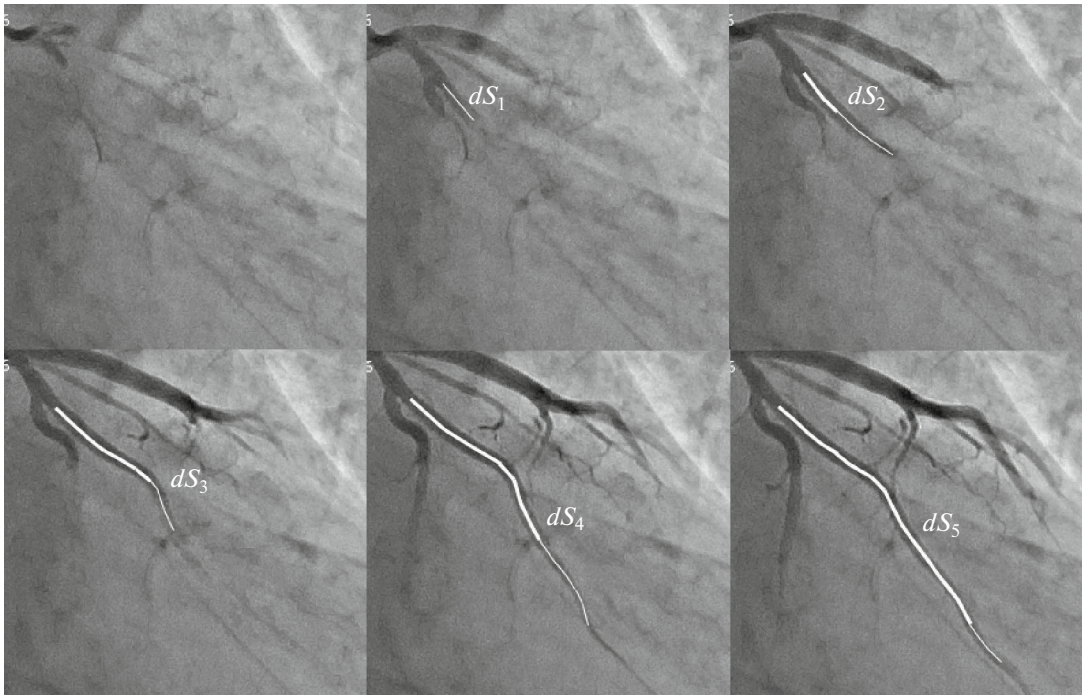


Fig. 7. Spread of the contrast agent through the coronary artery vessel after its injection into the mouth of the coronary arteries. dS_1-dS_5 is the path covered by the contrast agent in the corresponding frame (see explanations in the text).

the previous interframe interval. The figure qualitatively illustrates the stages of spread of the contrast agent through the artery. It quantitatively contains the information about the velocity of blood flow through the CA. The linear velocity v at the moment of time that corresponded to the frame “ i ” was calculated by the formula

$$v_i = \frac{dS_i}{\Delta t}, \quad (2)$$

where dS_i is the path covered by the contrast agent over the time interval between frames “ $i - 1$ ” and “ i ”; Δt is the interframe interval.

Thus, the algorithms considered in this section allowed us to quantitatively characterize the dynamics of the contrast agent in the coronary arteries, making allowance for the peculiarities of their visualization at various phases of the mechanical cardiac cycle. It should be added that the blood velocity was estimated precisely at the site of the artery where the contrast agent front was at that moment.

Estimation of Blood-Flow Velocity in Coronary Artery Stenosis Using a Specific Example

The developed algorithms for determining the geometry of the coronary arteries and estimating the velocity of spread of the radiopaque agent in them based on the angiographic research data were implemented as software in the “Delhi10.3 Community Edition” programming environment of the “Embar-

cadero” Company (free license). The initial data used were videotaped results of examinations of patients with coronary heart disease (CHD).

To give an example, Fig. 8 shows a studied coronary artery section with stenosis, and Fig. 9 shows the sequence of video frames during the period of the vessel being filled with the radiopaque agent. Figure 10 shows the results of estimating the diameter of the coronary artery based on angiograms recorded in two projections, which are rotated 30° relative to each other.

According to the data of Fig. 10, the stenotic area (at a distance of ~ 70 mm from the beginning of the studied CA section, see Fig. 9) has an approximately two-fold narrowing of the artery relative to its diameter in front of the stenosis (a distance of ~ 30 mm from the beginning of the studied section). The root-mean-square value of the difference in arterial diameters (a section of 60–80 mm) in the two projections in the stenotic area did not exceed 9.8% of the average value of the artery diameter in the same area in the 34° RAO projection.

Figure 11 presents the results of estimating the linear velocity of spread of the contrast agent for the considered case on the basis of two projections of coronarogram recording. It can be seen that the absolute values of the velocity differ for the two projections in the stenotic area of 60–80 mm. However, the ratio of the velocities at the site of stenosis (70 mm) and at its beginning (30 mm) differed by no more than 10% for

the two projections. In particular, the ratio of the velocities was approximately 2 for the 34° RAO projection and 1.8 for the 4° RAO projection. The root-mean-square value of the difference in blood-flow velocities through the stenosis area in the two projections did not exceed 12% of the average value of the blood-flow velocity in the same area in the 34° RAO projection. It should be noted that the limitations in the accuracy of the methods used did not permit us to detect velocity fluctuations at the narrowed site of the artery, which was located above the extended stenosis (see Figs. 8 and 10).

Having the information about the distribution of artery diameter and linear blood-flow velocity along the length of the vessel, one can estimate the volumetric blood-flow velocity Q . The volumetric blood-flow velocity Q for the frame “ i ” in the place of the artery where the contrast agent front is located can be calculated using the standard formula

$$Q_i = v_i A_i, \quad (3)$$

where A_i is the cross-sectional area of the vessel in this section and v_i is the linear blood-flow velocity calculated by formula (2).

Theoretically, the volumetric velocity of fluid flow through the vessel at the same time point does not depend on the spatial coordinate (if the vessel has no branches). However, in the proposed method, the linear velocity of spread of the contrast agent through the artery was estimated not only in different parts of the vessel, but also in different phases of the cardiac cycle. Accordingly, the obtained values of the volumetric blood-flow velocity have a certain scatter. To reduce the effect of the method's errors on the final result of the volumetric velocity calculations according to (3), the averaged value of Q over all video frames was used. For the data used above (see Figs. 10 and 11, 34° RAO projection), the following estimate of the volumetric blood-flow velocity over the artery section under study was obtained: 1.6 ± 0.6 mL/s ($p = 0.05$; $n = 7$).

Computer Simulation of Blood Flow in the Coronary Artery with Stenosis

The hemodynamic situation in the CA (see Fig. 8) was modeled using the computer simulation by the finite-element method, which makes it possible to obtain a numerical solution of differential nonlinear equations for a laminar fluid flow taking into account the topology and physicochemical parameters of the hydrodynamic system. This was done using a computer station based on the SuperMicro 4U 7047A-T server platform (United States) with 128 GB of RAM and 32 cores of an Intel XeonX5 CPU with a rate of 3.3 GHz. The simulation was carried out using the Comsol Multiphysics 5.4 licensed software (Sweden, license 17074991, core and Microfluidics module).

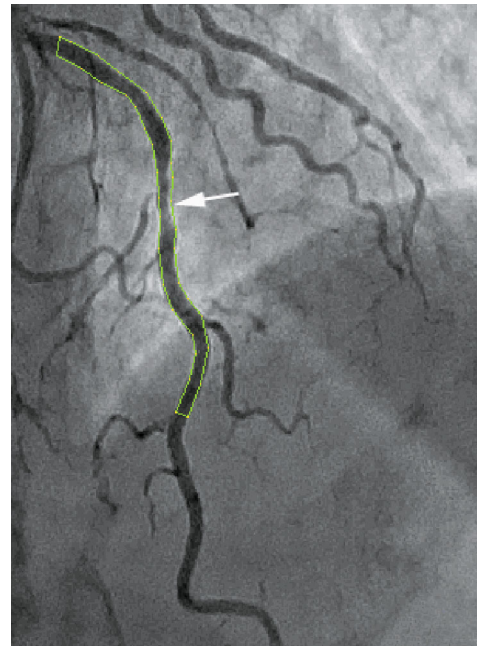


Fig. 8. (Color online) Example of a coronary artery site with a pronounced stenosis. The place of extensive stenosis in the middle third at the anterior interventricular branch of the left coronary artery is indicated by the arrow; 34° RAO projection.

The structure of the artery for the computer model was obtained from a video frame (see Fig. 8) using the pattern-recognition algorithms based on the Fourier analysis of the bitmap image and Bresenham's algorithms [21]. This problem was solved using an unstructured mesh of tetrahedral (a mesh with non-uniform coupling) and a generator of tetrahedral meshes based on the Delaunay algorithms [22]. Figure 12a shows a fragment of the artery at the border of the stenosis with a division of the vessel geometry on the tetrahedral with boundaries (from 0.004 to 0.025 mm). Mesh compression was chosen from the condition that the gradient of velocity depends on the distance from the axis of symmetry: the velocity gradients are small closer to the axis and largest near the vessel wall.

To solve the hemodynamic problem, a number of assumptions were used. The values of dynamic viscosity ($\eta = \text{const} = 0.00345$ Pa s) and density ($\rho = \text{const} = 1050$ kg/m³) of the fluid were set close to those of blood plasma. The influence of temperature on the viscosity of the fluid was not taken into account. It was assumed that the fluid was incompressible, that its viscosity did not depend on the gradient of velocity; i.e., a Newtonian fluid was considered. These assumptions reflect the properties of blood plasma, but do not strictly correspond to the properties of blood. The walls of the vessel and stenosis in the model were absolutely rigid due to the lack of real data on the rigidity of the artery and stenosis wall, which also depend on the

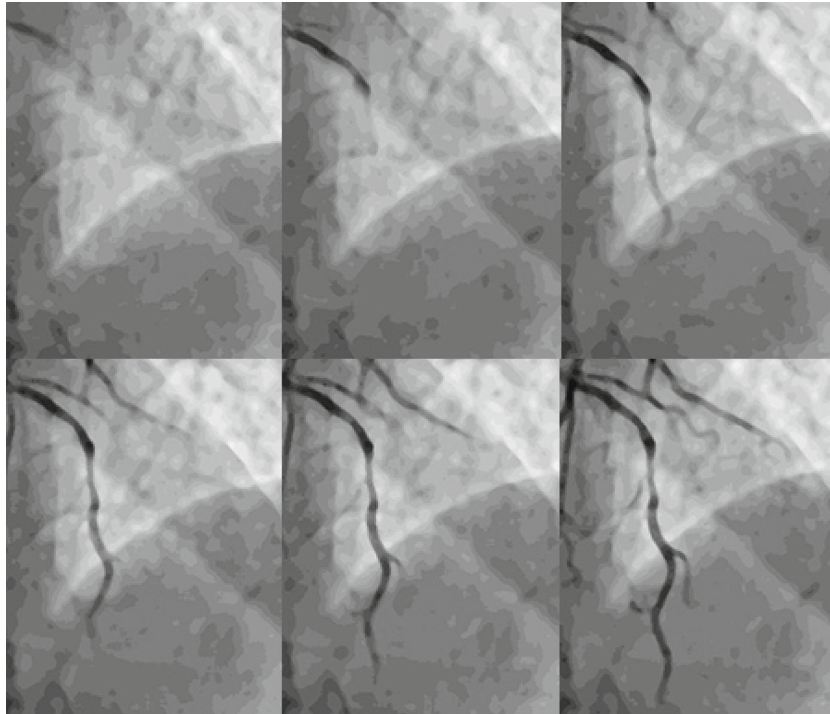


Fig. 9. The sequence of the frames detected during the period of the spread of the contrast agent through the artery section under study; 34° RAO projection.

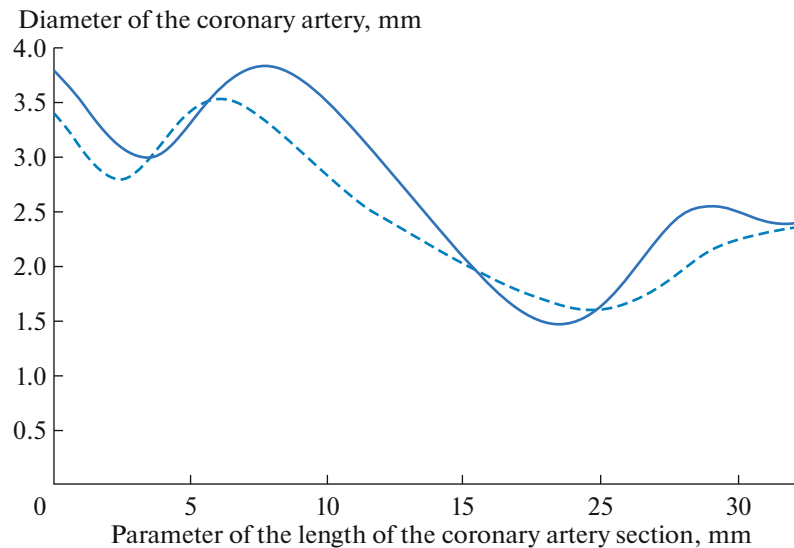


Fig. 10. (Color online) Distribution of the diameter of the coronary artery in the studied section. The solid line corresponds to 34° RAO projection; the dotted line corresponds to the 4° RAO projection.

functional state of the smooth muscles of the arterial wall. The aggregation properties were not taken into account either.

The blood flow in a bulk vessel was defined by the Navier-Stokes equations for a viscous incompressible fluid without a time parameter and by the continuity equation. Gravitational forces were not taken into

account. The “no-slip” boundary condition was applied [23], i.e., the condition of zero velocity on vessel walls:

$$\begin{aligned} \rho(\mathbf{V} \cdot \nabla)\mathbf{V} &= \nabla \cdot [-p + \eta(\nabla\mathbf{V} + (\nabla\mathbf{V})^T)], \\ \rho\nabla \cdot (\mathbf{V}) &= 0, \end{aligned} \quad (4)$$

where ρ is the density of the fluid, η is the dynamic viscosity of the fluid, p is the pressure, and \mathbf{V} is the velocity vector that has the components x and y . The conditions

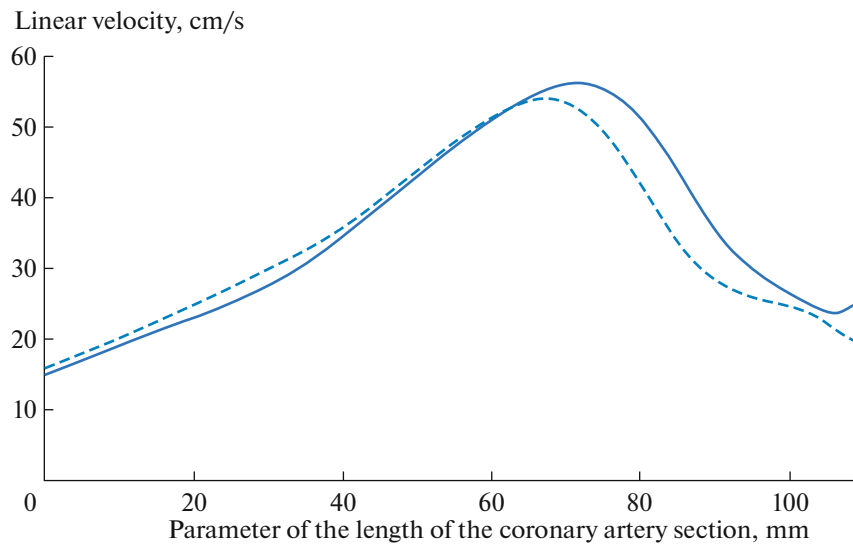


Fig. 11. (Color online) Distribution of the velocity of spread of the contrast agent through the coronary artery. The solid line corresponds to the 34° RAO projection; the dotted line corresponds to the 4° RAO projection.

that the flow must be parallel to the vessel axis were established for the velocities at the boundaries of the artery fragment. The initial flow velocity was 15 cm/s.

The systems of nonlinear equations in stationary and time-dependent conditions were solved using the Newton damped method [24], when the system is solved fully coupled. This method is based on the linearization of non-linear equations and solving of linear equations in a sequence of Newton iterations until we obtain the desired accuracy.

Figure 12b shows the color diagram of the distribution of the instantaneous velocity value over the mesh model of the CA. It can be seen that the fluid flow velocity is several times greater at the site of stenosis than before and after the narrowed site of the artery. The result obtained is qualitatively in good agreement with the results of measurements of the velocity of the contrast agent according to the angiographic data (see Fig. 11).

Throughout the CA, the perpendicular component of velocity to the section of the model artery area had a parabolic profile, indicating a laminar character of the flow. The initial laminar flow before the stenosis was observed to have a parabolic velocity distribution from 0 to 23 cm/s over a 3.5-mm-wide CA section. In the central area of the stenosis, the velocity distribution also had a parabolic profile, but the maximum velocity increased up to 37 cm/s. At the exit of the stenosis, i.e., in the area where the vessel drastically widened, the velocity profile became different from the parabolic one, which implies the presence of small eddy mixing zones in this area. Meanwhile, in the vessel area of 2–4 mm after the stenosis, the instantaneous velocity in the central part of the CA remained elevated (up to 30 cm/s).

In general, the results of computer simulation allowed us to demonstrate the complex hemodynamic situation in the artery with stenosis and showed the similarity with blood flow measurement data at the qualitative level using the method considered in the paper.

Sources of Errors, Ways to Minimize Them and Prospects for Using the Proposed Methodology

This paper presents the methodological techniques for estimating blood flow in the coronary arteries based on the analysis of heart video images recorded

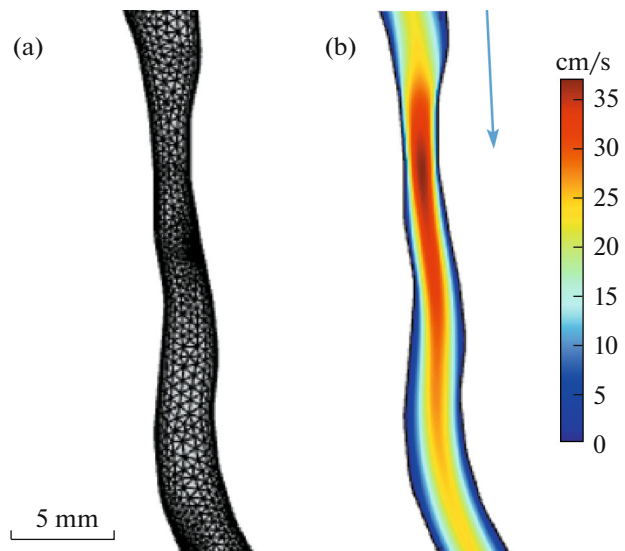


Fig. 12. (Color online) (a) Fragment of the mesh model of coronary artery. The section with stenosis is shown, which is indicated by the arrow in Fig. 8. (b) The distribution of the instantaneous velocity gradient in the stenotic area. The arrow shows the direction of blood flow.

during the standard angiographic examination of patients. It was necessary to solve the problem associated with the correct description of the velocity of spread of the radiopaque agent front in the initial period after the injection of the agent into the mouth of the coronary bed. It should be noted that a similar formulation of the problem has already been considered in a number of studies, the results of which have been published earlier [25–27].

The algorithms we use for analyzing heart video images have certain advantages. In particular, they allow the correction of the trajectory of spread of the contrast agent through the artery with consideration for the movement of the vessel and changes in its configuration due to the mechanical activity of the heart. For this purpose, the configuration of the studied CA section was initially determined in accordance with the phases of the cardiac cycle during the period of the best visualization of the arteries. The information obtained was used to more accurately determine the path covered by the contrast agent inside the artery. Ultimately, this provided the increased accuracy of calculating the linear and volumetric blood-flow velocities.

The ratio of the maximum velocity (in the center of a stenosis) to the minimum velocity (in front of the stenosis) characterizes the effect of the stenosis on the blood flow; i.e., it gives additional information for the choice of treatment tactics. In the usual case of small lengths of the stenotic artery sites (10–15 mm), the angle between the blood flow velocity vector and the angiographic projection plane is not known, but does not change significantly. This undoubtedly introduces an error in estimating the absolute values of the blood-flow velocity, but does not significantly affect the accuracy of determining the ratio of the velocities in front of the stenosis and in its center. This judgment was confirmed by presenting the data on measuring the blood-flow velocities in two projections, which were turned relative to each other at an angle of 30° . The difference in the velocities did not exceed 10% (see Fig. 11).

Despite the fact that testing of the algorithms on clinical material and comparison of their work with computer simulation data have shown quite realistic and promising results, the limitations of the proposed methodology have become obvious. Thus, at a video recording speed of 15 frames per second, the contrast agent can move by 10–20 mm over the interval between adjacent frames. Due to the rather large spatial discreteness in calculating the velocity of movement of the contrast agent, an artery section with stenosis can be overlooked. A comparison of the data in Figs. 10 and 11 illustrates this situation well. Therefore, the original data must be recorded at the maximum available speed. For instance, if the speed of video recording during an angiographic examination is 60 frames per second, the spatial discreteness of the obtained estimates is no more than 2–4 mm.

A certain source of errors is the accuracy of recording of the phases of the cardiac cycle. In the present study, the video images in different periods of contrasting of the arteries were bound to the frame which was the closest to the end of the heart diastole. To improve measurement accuracy, it is necessary to synchronize the recording of images with an electrocardiogram.

The most significant limitations of the proposed methodology are due to the lack of consideration for the three-dimensional orientation of the coronary arteries. This circumstance can be a source of significant errors in determining the size of the arteries and the velocity of movement of the contrast agent in them, especially in cases with complex stenoses of CAs. Within the framework of this study, we did not have the technical ability to compare the accuracy of the approach considered in the article with the results of CT or MRT. In principle, it is impossible to do this in the context of examining the same patient for obvious ethical reasons. A comparative assessment of the methods can be indirectly made on the basis of studies of other authors. For example, the study [28] used the CT method to estimate the accuracy of measuring the velocity of water in a model blood vessel in the form of a silicon tube. The average values of the relative errors were in the range of 13–26%.

Another paper [29] presents methods similar to ours for estimating the velocity of coronary blood flow from 2D-angiographic images with the injection of a contrast agent. In this study, the average linear blood-flow velocity was measured over a fairly long part of the artery (several centimeters), and the accuracy of the method was estimated using the data of intravascular dopplerometry (this is the most accurate method for measuring blood-flow velocity at the moment). According to the results of the examination of 21 patients, the authors found that the root-mean-square error in estimating coronary blood-flow velocity using their method was 35% relative to the reference method.

Thus, the accuracy of estimating coronary blood-flow velocity according to 2D coronarograms is approximately 35% versus the accuracy of 13–26% in the case of using 3D computed tomography data. We believe that the difference in accuracy between the methods is quite acceptable, making allowance for the differences in price and the degree of availability of the considered methods.

Meanwhile, with consideration for the listed limitations, the proposed methodical techniques can be useful for solving a number of urgent problems of interventional cardiology. Thus, the algorithm for frame-by-frame determination of the boundaries and configuration of CAs over a single cardiac cycle allows constructing a video pattern of the coronary bed with consideration for the features of visualization of the arteries in different phases of the mechanical cardiac cycle. This will make it possible to perform surgical

manipulations in balloon angioplasty and stenting of CAs without the injection of a radiopaque agent. This function, which is called the “Roadmap,” is widely used for stenting of peripheral arteries that are not very mobile or completely immobile [30].

The considered methods provide additional information about the hemodynamic significance of stenosis of a CA, i.e., about the contribution of atherosclerotic artery constriction to the blood supply to the myocardium. Such information is necessary to select the tactics and scope of treatment of patients with coronary heart disease. Today, the most accurate information on the significance of stenosis can be obtained by the methods of intravascular ultrasound examination and/or intravascular manometry. The latter method, which is called “Fractional Flow Reserve (FFR)” [31], operates with pressure measurement results before and after the narrowed site of a CA, on the basis of which the flow velocity gradient is determined. The same information can be obtained with a certain degree of accuracy using the proposed methodology, moreover, in the course of a standardized angiographic study of patients without the use of expensive equipment.

In addition, the proposed algorithms for describing the movement of the front of the contrast agent in the period immediately after its injection into the mouth of the coronary arteries can be successfully applied to estimate the rate of the contrast agent moving out from the heart. Such information has an important prognostic value for a number of clinical cases [6].

In general, the preliminary research results presented in the paper contain a certain potential for the introduction of the considered methods into clinical practice for the needs of modern cardiology. It is important that the considered algorithms are focused on increasing the diagnostic value of the most common and routine method of interventional examination and treatment of patients with coronary heart disease.

ACKNOWLEDGMENTS

The authors thank D.Yu. Tobolin for critical comments and recommendations in the preparation of the article.

FUNDING

The studies on computer modeling of hemodynamics in the coronary arteries were financially supported by grant of the Russian Science Foundation no. 18-19-00090.

COMPLIANCE WITH ETHICAL STANDARDS

Conflict of interests. The authors declare that they have no conflict of interest.

Statement of compliance with standards of research involving humans as subjects. This article does not contain any research involving human subjects as research objects.

REFERENCES

1. F. J. Neumann, M. Sousa-Uva, A. Ahlsson, F. Alfonso, A. P. Banning, U. Benedetto, et al., “2018 ESC/EACTS Guidelines on myocardial revascularization,” *Eur. Heart J.* **40** (2), 87–165 (2018).
2. R. J. Gibbons, W. S. Weintraub, and R. G. Brindis, “Moving from volume to value for revascularization in stable ischemic heart disease: A review,” *Am. Heart J.* **204**, 178–185 (2018).
3. S. Tu, E. Barbato, et al., “Fractional flow reserve calculation from 3-dimensional quantitative coronary angiography and TIMI frame count: A fast computer model to quantify the functional significance of moderately obstructed coronary arteries,” *JACG: Cardiovasc. Interv.* **7** (7), 768–777 (2014).
4. S. S. Nijjer, G. A. de Waard, S. Sen, T. P. van de Hoef, R. Petraco, et al., “Coronary pressure and flow relationships in humans: phasic analysis of normal and pathological vessels and the implications for stenosis assessment: A report from the Iberian–Dutch–English (IDEAL) collaborators,” *Eur. Heart J.* **37** (26), 2069–2080 (2016).
5. D. J. Duncker, A. Koller, D. Merkus, and J. M. Canty Jr., “Regulation of coronary blood flow in health and ischemic heart disease,” *Prog. Cardiovasc. Dis.* **57** (5), 409–422 (2015).
6. S. Vijayan, D. S. Barmby, I. R. Pearson, A. G. Davies, S. B. Wheatcroft, and M. Sivanathan, “Assessing coronary blood flow physiology in the cardiac catheterisation laboratory,” *Curr. Cardiol. Rev.* **13** (3), 232–243 (2017).
7. C. J. Arthurs, K. D. Lau, K. N. Asrress, S. R. Redwood, and C. A. Figueroa, “A mathematical model of coronary blood flow control: Simulation of patient-specific three-dimensional hemodynamics during exercise,” *Am. J. Physiol. Heart Circ. Physiol.* **310** (9), H1242–H1258 (2016).
8. S. Molloy, D. Chalyan, H. Le, and J. T. Wong, “Estimation of coronary artery hyperemic blood flow based on arterial lumen volume using angiographic images,” *Int. J. Cardiovasc. Imaging* **28** (1), 1–11 (2012).
9. L. G. Shapiro and G. C. Stockman, *Computer Vision* (Prentice Hall, Upper Saddle River, NJ, 2001; Binom, Moscow, 2006).
10. D. S. D. Lara, A. W. C. Faria, A. de A. Araújo, and D. Menotti, “A novel hybrid method for the segmentation of the coronary artery tree in 2D angiograms,” *Int. J. Comput. Sci. Inf. Technol. (IJCSIT)* **5** (3), 45–65 (2013).
11. M. N. Dehkordi, S. Sadri, and A. Doosthoseini, “A review of coronary vessel segmentation algorithms,” *J. Med. Signals Sens.* **1** (1), 49–54 (2011).
12. I. Cruz-Aceves, A. Hernandez-Aguirre, and I. Valdez-Peña, “Automatic coronary artery segmentation based on matched filters and estimation of distribution algorithms,” in *Proc. 19th Int. Conf. on Image Processing, Computer Vision, and Pattern Recognition (ICCV’15)* (Las Vegas, NV, 2015), pp. 405–410.
13. S. Yu. Sokolov, A. A. Grinko, A. V. Tourovskaia, F. B. Reitz, O. Yakovenko, G. H. Pollack, and F. A. Blyakhman, “Minimum average risk” as a new peak-detection algorithm applied to myofibrillar dy-

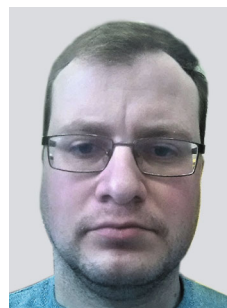
- namics,” *Comput. Methods Programs Biomed.* **72** (1), 21–26 (2003).
14. M. Kass, A. Witkin, and D. Terzopoulos, “Snakes: Active contour models,” *Int. J. Comput. Vision* **1** (4), 321–331 (1988).
 15. X. Bresson, P. Vandergheynst, and J.-P. Thiran, “Multiscale active contours,” *Int. J. Comput. Vision* **70** (3), 197–211 (2006).
 16. A. Zifan, P. Liatsis, P. Kantartzis, M. Gavaises, N. Karcianas, and D. G. Katritsis, “Automatic 3D reconstruction of coronary artery centerlines from monoplane X-ray angiogram images,” *Int. J. Biol. Med. Sci.* **2** (3), 105–110 (2008).
 17. S. Yu. Sokolov and F. A. Blyakhman, “A method for automatic delineation of the left ventricle borders in echographic images with use active contours and speckle tracking techniques,” in *The 15th International Conference on Biomedical Engineering, ICBME 2013*, Ed. by J. Goh, IFMBE Proceedings (Springer, Cham, 2014), Vol. 43, pp. 76–79.
 18. S. Yu. Sokolov, “Improving the accuracy and stability of the speckle tracking technique in processing images obtained in echocardiographic examinations,” *Pattern Recogn. Image Anal.* **23** (4), 536–540 (2013).
 19. Yu. A. Zinovyeva, K. R. Mekhdiya, S. Yu. Sokolov, and F. A. Blyakhman, “Mapping of false tendons in the left ventricle based on the heart transthoracic ultrasound visualization,” *J. Med. Imaging Health Inf.* **5** (6), 1217–1222 (2015).
 20. S. Yu. Sokolov, “Assessment of peristaltic movements of the intestine by the method of tracking of specific areas of the video obtained at surgery,” in *Proc. 2012 5th Int. Conf. on Biomedical Engineering and Informatics (BMEI 2012)* (Chongqing, China, 2012), IEEE, pp. 212–215.
 21. L. Ammeraal and K. Zhang, *Computer Graphics for Java Programmers*, 2nd ed. (Wiley, Chichester, 2007).
 22. A. J. Baker, *Finite Elements: Computational Engineering Sciences*, 1st ed. (Wiley, Chichester, 2012).
 23. D. W. Pepper and J. C. Heinrich, *The Finite Element Method: Basic Concepts and Applications*, 2nd ed. (Taylor & Francis, CRC Press, Boca Raton, 2005).
 24. R. W. Pryor, *Multiphysics Modeling Using COMSOL®: A First Principles Approach*, 1st ed. (Jones and Bartlett Publ., Burlington, 2009).
 25. J. Y. Goulermas and P. Liatsis, “Hybrid symbiotic genetic optimization for robust edge-based stereo correspondence,” *Pattern Recogn.* **34** (12), 2477–2496 (2001).
 26. P. Windyga, M. Garreau, M. Shah, H. Le Breton, and J. L. Coatrieux, “Three-dimensional reconstruction of the coronary arteries using a priori knowledge,” *Med. Biol. Eng. Comput.* **36** (2), 158–164 (1998).
 27. N. Yu. Ilyasova, N. L. Kazansky, A. O. Korepanov, A. V. Kupriyanov, A. V. Ustinov, and A. G. Khrarov, “Computer technology for the spatial reconstruction of the coronary vessels structure from angiographic projections,” *Komp. Optika (Comput. Opt.)* **33** (3), 281–317 (2009) [in Russian].
 28. S. Prevrhal, C. H. Forsythe, R. J. Harnish, M. Saeed, and B. M. Yeh, “CT angiographic measurement of vascular blood flow velocity by using projection data,” *Radiol.* **261** (3), 923–929 (2011).
 29. M. Khanmohammadi, K. Engan, C. Sæland, T. Eftestøl, and A. I. Larsen, “Automatic estimation of coronary blood flow velocity step 1 for developing a tool to diagnose patients with micro-vascular angina pectoris,” *Front. Cardiovasc. Med.* **6**, 1–11 (2019). <https://doi.org/10.3389/fcvm.2019.00001>
 30. *Practical Peripheral Vascular Intervention*, 2nd ed., Ed. by I. P. Casserly, R. Sachar, and J. S. Yadav, (Lippincott Williams and Wilkins, Philadelphia, 2011).
 31. C. Shi, D. Zhang, K. Cao, et al., “A study of noninvasive fractional flow reserve derived from a simplified method based on coronary computed tomography angiography in suspected coronary artery disease,” *Biomed. Eng. Online* **16** (1), 43, 1–15 (2017). <https://doi.org/10.1186/s12938-017-0330-2>

Translated by L. Solovyova



Sokolov Sergei Yur'evich. Born in 1961. Graduated from the Radio Engineering Faculty of Ural Polytechnic Institute (Sverdlovsk, 1984), candidate of physical and mathematical sciences (2000), assistant professor (2010). Head of the Department of Medical Physics, Informatics and Mathematics, senior researcher of the Department of Biomedical Physics and Engineering at Ural State Medical University (Yekaterinburg), lecturer at

the Institute of Natural Sciences and Mathematics of Yeltsin Ural Federal University (Yekaterinburg). Scope of scientific interests: digital signal- and image-processing, signal-filtering issues, hardware and algorithmic support of biomedical research. Author of 35 publications and a monograph chapter, two patents for invention, winner of 5 awards and prizes for the results of professional activities.



Volchkov Stanislav Olegovich. Born in 1982. Graduated from the Physics Department of Gorky Ural State University (Yekaterinburg, 2006), candidate of physical and mathematical sciences (2009). Senior researcher at the Institute of Natural Sciences and Mathematics of Yeltsin Ural Federal University (Yekaterinburg) and the Department of Biomedical Physics and Engineering of Ural State Medical University (Yekaterinburg). Scope of scientific

interests: magnetic-field sensors, high-frequency circuitry, object-oriented programming. Author of 38 publications, member of the International Association of Electrical and Electronics Engineers (IEEE), winner of 4 awards and prizes for the results of professional activities.



Bessonov Ivan Sergeevich. Born in 1984. Graduated from the Medical Faculty of the Tyumen State Medical Academy (2007), candidate of medical sciences (2013). Head of the laboratory of X-ray endovascular methods of diagnosis and treatment at the Tyumen Cardiology Research Center (Tomsk National Research Medical Center of the Russian Academy of Sciences). Scope of scientific interests: interventional cardiology. Author of 59 publications,

member of the Russian and European Society of Cardiology and European Association for Percutaneous Coronary Interventions.



Kurlyandskaya Galina Vladimirovna. Born in 1961. Graduated from the Faculty of Physics of Gorky Ural State University (Sverdlovsk, 1983), doctor of physical and mathematical sciences (2007). Professor at the Institute of Natural Sciences and Mathematics, leading researcher of the Research Institute of Physics and Applied Mathematics, Magnetism and Magnetic Nanomaterials of Yeltsin Ural Federal University (Yekaterinburg). Scope of scientific

interests: theoretical and experimental physics of magnetic phenomena and materials, biosensorics, nanotechnology for biomedical applications. Author of 10 collective monographs and textbooks, 245 journal articles, several patents for inventions. Member of a number of scientific societies and program committees of conferences, editorial boards of two journals.



Chestukhin Vasilii Vasil'evich. Born in 1941. Graduated from Sechenov First Moscow Medical Institute (1965), doctor of medical sciences (1994), professor (1996). Scientific consultant of Sklifosovsky Research Institute of Emergency Care (Moscow). Scope of scientific interests: clinical physiology and pathophysiology of the heart. Author of 3 collective monographs, more than 300 publications, several patents for inventions. Member of the editorial

board of the international journal "Interventional Cardiology," laureate of the Prize of the Government of the Russian Federation, Honored Doctor of Russia.



Blyakhman Feliks Abramovich. Born in 1957. Graduated from the Faculty of Biology of Gorky Ural State University (Sverdlovsk, 1979), doctor of biological sciences (1996), professor (2002). Head of the Department of Biomedical Physics and Engineering at Ural State Medical University (Yekaterinburg), professor at the Institute of Natural Sciences and Mathematics of Yeltsin Ural Federal University (Yekaterinburg). Scope of scientific interests: physiology and

biophysics of muscular systems, biomimetics, medical physics and tissue engineering. Author of 9 collective monographs and textbooks, more than 100 journal articles, 11 patents for inventions. Member of a number of scientific societies and program committees of conferences, laureate of various awards and prizes for results of professional activities.